chemistry

MDPI

Article

Low-Molecular-Weight Versus Protein Inhibitors for the CXCL8/Glycosaminoglycan Interaction: Biophysical Characterization and Cellular Activity

Tanja Gerlza [1], Paula Peinsipp [1], Birgit Müller [1], Klaus Thirring [2] and Andreas J. Kungl [1,3,*]

[1] Institute of Pharmaceutical Sciences, University of Graz, Schubertstraße 1, A-8010 Graz, Austria; tgerlza@gmail.com (T.G.); paula.peinsipp@uni-graz.at (P.P.)
[2] Novartis Forschungsinstitut, Brunnerstrasse 59, A-1235 Vienna, Austria
[3] Antagonis Biotherapeutics GmbH, Strasserhofweg 77a, 8045 Graz, Austria
* Correspondence: andreas.kungl@uni-graz.at

Abstract

CXCL8, a pro-inflammatory chemokine, which can be induced by TNF-α or IL-1, is responsible for the recruitment and activation of neutrophils. Chemokines interact with glycosaminoglycans on endothelial cells and are thus protected from degradation and sequestration, holding them in an optimal position for recruiting immune cells. Inhibiting the interaction of chemokines with their glycosaminoglycan co-receptors represents an attractive approach for the treatment of chemokine-mediated diseases. Two polyketide-pyrone compounds, PA501 and PA502 were synthesized, which bind to CXCL8 with affinities higher than the natural glycosaminoglycan ligand heparan sulfate, and in a similar range as heparin. Significant structural changes were induced in the chemokine by interacting with the two compounds, as expressed in fluorescence and far-UV CD experiments. In filter binding assays, both compounds were found to displace heparan sulfate efficiently from CXCL8, with PA501 displaying the highest competition efficacy. Using a C-terminally truncated form of the chemokine, CXCL81-58, which lacks the main glycosaminoglycan-binding α-helical domain, the two compounds are suggested to use—to a varying degree—different binding sites on the protein, which have also been proposed for the natural heparan sulfate ligand. In a transmigration assay, PA501 and PA502 exhibited dose-dependent modulation of CXCL8-induced neutrophil mobilization and migration. The compounds PA501 and PA502 may thus be regarded as early novel lead compounds in the quest for anti-inflammatory, chemokine-targeting drugs.

Keywords: chemokines; glycosaminoglycans; inflammation; transmigration; proteoglycans; CXCL8

Check for updates

Academic Editors: Igor Alabugin and Juan B. Rodriguez

Received: 15 March 2026
Revised: 5 June 2026
Accepted: 8 June 2026
Published: 10 June 2026

Copyright: © 2026 by the authors. Licensee MDPI, Basel, Switzerland. This article is an open access article distributed under the terms and conditions of the Creative Commons Attribution (CC BY) license.

1. Introduction

IL-8, or CXCL8, is a pro-inflammatory C-X-C chemokine, which exhibits neutrophil chemotactic activity. CXCL8 can be induced by pro-inflammatory stimuli, such as IL-1 and tumor necrosis factor-α (TNF-α) by various types of cells, e.g., monocytes, T-cells, natural killer cells, stromal cells, epithelial cells, dermal fibroblasts, hepatocytes, and keratinocytes [1–4]. It has been detected at various inflammatory sites, setting up a chemotactic gradient for neutrophils and transforming the selectin-mediated process of leukocyte rolling on the endothelium into an integrin-mediated process, resulting in firm adherence and extravasation of the leukocytes [5,6]. CXCL8 exerts its function by interacting with

chemokine receptors CXCR1 and CXCR2 on leukocytes, mediating leukocyte trafficking during infections, which results in transmigration along the endothelium to sites of inflammation [7–9]. CXCL8 consists of 99 amino acids and belongs to the family of CXC chemokines. After cleavage of the signal peptide, there are two primary forms, which are 77 or 72 amino acids, whereby the latter is more biologically relevant [5,10,11]. Glycosaminoglycans, which are present on the endothelium, are important co-receptors because, due to the polyanionic character of the glycsoaminoglycans (GAGs) and the basic nature of chemokines, they exhibit a strong binding that facilitates the concentration of chemokines on the cell surface and further protects them from sequestration and degradation [12]. Glycosaminoglycans are unbranched linear, sulphated, anionic polysaccharides composed of repeating disaccharide units. There are different groups of GAGs, which differ in the type of hexosamine (D-glucosamine, or D-galactosamine), the uronic acid (glucuronic, iduronic), the geometry of the glycoside linkage (α- or β-), as well as the relative position (1→3, 1→4) [13–16]. The main classes are (1) hyaluronic acid, (2) chondroitin sulfate, (3) dermatan sulfate, (4) heparin, (5) heparan sulfate, and (6) keratan sulfate. Glycosaminoglycans, except hyaluronic acid, are sulfated at various positions and are attached to core proteins, forming the so-called proteoglycans [13,17]. A plethora of cells produce proteoglycans, and they can be either inserted into the plasma membrane, stored in secretory granules, or secreted into the extracellular matrix (ECM). Proteoglycans can be substituted with one or two types of glycosaminoglycans, e.g., syndecan-1 has attached heparan sulfate (HS) and chondroitin sulfate (CS) chains [18]. Proteoglycans are part of the extracellular matrix and are seen as the "backbone" of the glycocalyx, representing a part of the outer membrane of the vascular endothelium on the luminal side [19]. It has a dynamic network of glycoproteins and proteoglycans that permits soluble endothelium and plasma-derived compounds to be integrated. This carbohydrate-rich layer (thickness 0.5 to 1 μm) is difficult to quantify and should not be viewed as a static structure because it continually shifts between GAG shedding and biosynthesis [20]. Many proteoglycans have various actions, whereas others have specific intracellular functions. Proteoglycans are engaged in endocytosis and degradation processes and facilitate the extremely dynamic interplay between cells, neighboring structures, and matrix [15,21,22].

Heparan sulfate is the most widely distributed member of the glycosaminoglycan family, and it is characterized by a linear chain of 10–200 disaccharide units; it has numerous sequence motifs and is ubiquitously expressed on cell surfaces and in the extracellular matrix of vertebrate and invertebrate species [23,24]. It is a polyanionic linear polysaccharide formed in the Golgi apparatus of almost every eukaryotic cell as a copolymer of alternating L-N-acetylglucosamine (GlcNAc) and D-glucuronic acid residues (GlcA) [25]. Both saccharides can be subjected to various modifications, including N-sulfation of the glycosamine and C6 epimerization of the glucuronic acid into iduronic acid (IdoA). Further, non-random and incomplete O-sulfation occurs at C2 of the uronic acid, and C6 and, rarely, at C3 of $GlcNSO_3$ and GlcNAc, thereby creating a vast variety of sequences [26]. Compared to the high sulfation degree of heparin, HS has regions with highly sulfated regions (S-domains), predominantly Ido-A sulphated, which are followed by sequences with GlcA-GlcNAc (acetylated glucosamine), and there are mixed domains (NA domains) [27,28]. For CXCL8/GAG interactions, acetylated spacers or mixed domains, which are around 14 monosaccharide units, contribute to the appropriate folding of the monomer in an antiparallel configuration when the two S-domains of HS, consisting of six monosaccharide units, simultaneously interact with CXCL8 [15,29]. The interaction between CXCL8 and HS is established through electrostatic forces between the basic regions of the chemokine and the negative charge of the GAG. The binding of GAGs to proteins is further driven by hydrogen bonding and Van der Waals interaction, with both forces contributing to speci-

ficity [30]. GAGs mainly interact with amino acids, which are exposed on the surface of the protein, and the amino acids Asn, Asp, Glu, Gln, Arg, His, and Trp are more likely to be involved in binding events. The consensus sequence for GAG binding proteins is XBBXBX and XBBBXXBX (B representing a basic amino acid). Still, due to their three-dimensional fold, the presented amino acids on the surface can be in close proximity but lie far apart in the amino acid sequence [15,22,30,31]. GAG binding sites of CXCL8 were reported to be Arg60, Lys64, Lys67, and Arg68, which are contained within the C terminal helix of the chemokine, as well as His18 and Lys20—contained in the proximal loop [32].

Since CXCL8 is an essential mediator of tissue damage in acute and chronic inflammation, inhibition of the CXCL8/GAG interaction represents an attractive approach to inhibiting inflammatory processes. Our group has previously designed a CXCL8-based dominant-negative mutant (dnCXCL8) with increased GAG binding affinity and with impaired GPC receptor (CXCR1/2) activity. This mutant was already tested in several mouse models for its anti-inflammatory potency and was used in this study to compare transmigratory inhibition of two novel synthetic polyketide-pyrone compounds [33–37]. These compounds have been chemically synthesized and were shown to interact with wildtype CXCL8 in a similar manner as heparin and HS, thereby inducing similar structural changes of the protein as induced by the natural ligands. Here we investigated the binding and displacement profile of these compounds, as well as their modulation potency of CXCL8-induced neutrophil chemotaxis and endothelial cell transmigration. Therefore, we propose that these substances could be of potential interest for a therapeutic approach for CXCL8-mediated diseases, as well as representing general alternatives for typical GAG-mimetics.

2. Materials and Methods

All materials, unless stated otherwise, were purchased from Sigma Aldrich (Merck, Darmstadt, Germany).

2.1. Preparative Synthesis of PA501 and PA502

All reactions were run at ambient temperature under argon. ^{1}H-NMR spectra were recorded on a Bruker WM 250 and DRX 500 spectrometer (Bruker, Billerica, MA, USA). Chemical shifts are quoted in parts per million downfield from TMS. Splitting patterns were designated as s (singlet), d (doublet), dd (doubled doublet), and m (multiplet). Mass spectra were run on a Finnigan Thermoquest Navigator LC-MS instrument (ThermoScientific, Waltham, MA, USA) in the ESI mode. Chromatography uses silica gel (Merck 0.05–0.2 mm) and Merck columns to medium-pressure column chromatography. The fungal metabolite 1 (originally discovered at Sandoz Basle, AG, Basel, Switzerland; unpublished results) was provided by Biochemie Kundl, Tirol, Austria. The structure of the obtained polyketide-pyrone compounds is depicted in Figure 1.

Acetic acid (2E,4E,10E,12E)-7-acetoxy-1-[1-((2R,3R,4R,6R)-3,4-diacetoxy-4′-hydroxy-6-hydroxymethyl-2′-oxo-3,4,5,6-tetrahydro-2.H.,2′.H.-[2,3′]bipyranyl-6′-yl)-1-methyl-ethyl]-4,6,8,12,14,16-hexamethyl-octadeca-2,4,10,12-tetraenyl ester (2)

A total of 5 g (7.66 mmol) of (2R,3S,4R,6R)-6′-((3E,5E,11E,13E)-2,8-Dihydroxy-1,1,5,7,9,13,15,17-octamethyl-nonadeca-3,5,11,13-tetraenyl)-3,4,4′-trihydroxy-6-hydroxymethyl-3,4,5,6-tetrahydro-2.H.-[2,3′]bipyranyl-2′-one (**1**) were dissolved in 25 mL of pyridine and 25 mL of acetic anhydride. After stirring for 18h, the solvent was evaporated, the residue dissolved in toluene and pyridinium salts were filtered off. After solvent evaporation the residue was dissolved in 100 mL of methanol, 4 mL of 33% aqueous NH_3 were added and stirred for 18 h. Evaporation of the solvent and chromatography (CH_2Cl_2/MeOH 20:1) yielded 4.74 g (76%) of **2** ^{1}H-NMR ($CDCl_3$/CD_3OD 4:1) 6.30 (d, 1H, H_3, J = 15 Hz); 6.20

(d, 1H, H_{11}, J = 15.5 Hz); 5.91 (s, 1H, $H_{5'}$); 5.37–5.58 (m, 4H, $H_{1,2,5,10}$); 5.08–5.20 (m, 3H, $H3_{\text{-pyranyl,4-pyranyl,13}}$); 4.82 (d, 1H, H2-pyranyl, J = 9.4 Hz); 4.75 (dd, 1H, H-7, J = 4.4,7.8 Hz); 3.70–3.85 (m, 2H, $H_{\text{a-acetoxymethyl}}$, $H_{\text{b-acetoxymethyl}}$); 3.61 (m, 1H, $H_{\text{6-pyranyl}}$); 2.88 (m, 1H, H_6); 2.58 (m, 1H, H-14); 2.24 (m, 1H, H-$5_{\text{a-pyranyl}}$); 2.20 (m, 1H, H_{9a}); 2.08 (s, 3H, $COCH_3$), 2.04 (s, 3H, $COCH_3$); 2.01 (s, 3H, $COCH_3$), 2.00 (s, 3H, $COCH_3$); 1.83 (m, 1H, H_{9b}); 1.73–1.77 (m, 2H, $H5_{\text{b-pyranyl}}$, H8); 1.73 (2xs, 6H, $CH_{3\text{-}4,12}$); 1.17–1.30 (m, 3H, $H_{15a,16,17a}$); 1.24 (s, 3H, gem-CH_3); 1.21 (s, 3H, gem-CH_3); 1.05–1.18 (m, 2H, $H_{15b,17b}$); 0.98 (d, 3H, $CH_{3\text{-}6}$, J = 7 Hz); 0.93 (d, 3H, $CH_{3\text{-}14}$, J = 7 Hz); 0.80–0.88 (m, 9H, $CH_{3\text{-}8,16,18}$); MS-ESI *m*/*e* 829 (MH+, 100).

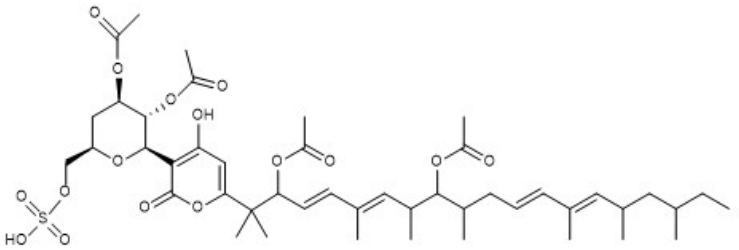

PA501

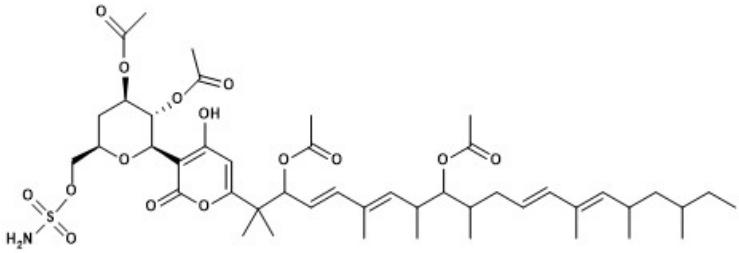

PA502

Figure 1. Structures of PA501 and PA502.

Acetic acid (2E,4E,10E,12E)-7-acetoxy-1-[1-((2R,3R,4R,6R)-3,4-diacetoxy-4′-hydroxy-2′-oxo-6-sulfooxymethyl-3,4,5,6-tetrahydro-2.H.,2′.H.-[2,3′]bipyranyl-6′-yl)-1-methyl-ethyl]-4,6,8,12,14,16-hexamethyl-octadeca-2,4,10,12-tetraenyl ester (3)

To 1 g of **2** (1.2 mmol) in 90 mL of DMF, 953 mg of SO_3-pyridine complex (6 mmol) was added and the resulting solution stirred for 12 h. After evaporation of the solvent with the help of added toluene the residue was purified by chromatography (CH_2Cl_2/MeOH 10:1), yielding 480 mg (44%) of **3**. 1H-NMR ($CDCl_3$/CD_3OD 4:1, 330K) 6.28 (d, 1H, H_3, J = 15.5 Hz); 6.03 (d, 1H, H_{11}, J = 15.4 Hz); 5.75 (s, 1H, $H_{5'}$); 5.56 (d, ^{1}H, H_1, J = 7.6 Hz); 5.50 (d, 1H, H_5, J = 7.5 Hz); 5.44–5.48 (m, 3H, $H_{3\text{-pyranyl}}$,2,10); 5.14 (m, 1H, $H_{\text{4-pyranyl}}$); 5.12 (d, 1H, H_{13}, J = 9.6 Hz); 4.87 (d, 1H, $H_{\text{2-pyranyl}}$, J = 11.1 Hz); 4.77 (dd, ^{1}H, H_7, J = 5.3,6.9 Hz); ABX-system (υA = 4.37, $H_{\text{a-acetoxymethyl}}$, υ_B = 4.08, $H_{\text{b-acetoxymethyl}}$, υX = 4.02, $H_{\text{6-pyranyl}}$, JAB = 10.9, JAX = 3.0, JBX = 1.9 Hz); 2.89 (m, 1H, H_6); 2.55 (m, 1H, H_{14}); 2.24 (m, 1H, H_{9a}); 2.20 (m, 1H, $H_{\text{5a-pyranyl}}$); 2.12 (m, 1H, $H_{\text{5b-pyranyl}}$); 2.05 (s, 3H, $COCH_3$), 2.02 (2xs, 6H, $COCH_3$); 1.90 (m, 1H, H_{9b}); 1.87 (s, 3H, $COCH_3$); 1.80 (m, 1H, H_8); 1.72 (2xs, 6H, $CH_{3\text{-}4,12}$); 1.22–1.30 (m, 3H, $H_{15a,\ 16,\ 17a}$); 1.23 (s, 3H, gem-CH_3); 1.18 (s, 3H, gem-CH_3); 1.13 (m, 1H, H_{17b}); 1.08 (m, 1H, H_{15b}); 0.95 (d, 3H, $CH_{3\text{-}6}$, J = 6.9 Hz); 0.93 (d, 3H, $CH_{3\text{-}15}$, J = 6.7 Hz); 0.82–0.87 (m, 9H, $CH_{3\text{-}8,16,18}$); MS-ESI *m*/*e* 947 (MK+, 100).

Acetic acid (2E,4E,10E,12E)-7-acetoxy-1-[1-((2R,3R,4R,6R)-3,4-diacetoxy-4′-hydroxy-2′-oxo-6-sulfamoyloxymethyl-3,4,5,6-tetrahydro-2.H.,2′.H.-[2,3′]bipyranyl-6′-yl)-1-methyl-ethyl]-4,6,8,12,14,16-hexamethyl-octadeca-2,4,10,12-tetraenyl ester (4)

To 600 mg of **2** (0.72 mmol) in 18 mL of DMF, 36 mg of NaH (1.5 mmol) was added and stirred for 45 min. A total of 432 mg (3.74 mmol) of $ClSO_2NH_2$ (prepared from chlorosulfonyl isocyanate and formic acid) were added and the resulting orange solution was stirred for a further 2 h. After evaporation of the solvent the residue was dissolved in ethyl acetate, washed with saturated sodium bicarbonate, brine and dried over magnesium sulfate. Chromatography (CH_2Cl_2/MeOH 20:1) yielded 375 mg (57%) of **4**. ^{1}H-NMR ($CDCl_3$/CD_3OD 4:1) 6.26 (d, 1H, H_3, J = 15.5 Hz); 6.03 (d, 1H, H_{11}, J = 15.5 Hz); 5.77 (s, 1H, $H_{5'}$); 5.74 (m, 1H, $H_{3\text{-pyranyl}}$) 5.57 (d, 1H, H_1, J = 7.5 Hz); 5.43–5.50 (m, 2H, $H_{2,10}$); 5.47 (d, 1H, H_5, J = 7.8 Hz); 5.10 (d, 1H, H_{13}, J = 9.3 Hz); 5.09 (m, 1H, $H_{4\text{-pyranyl}}$); 4.80 (m, 1H, $H_{2\text{-pyranyl}}$); 4.76 (dd, 1H, H_7, J = 4.6,7.6 Hz); ABX-system (υ¬A = 4.37, $H_{a\text{-acetoxymethyl}}$, υ¬B = 4.20, $H_{b\text{-acetoxymethyl}}$, υ¬X = 3.90, $H_{6\text{-pyranyl}}$, JAB = 11.9, JAX = 2.5, JBX = 4.6 Hz); 2.90 (m, 1H, H_6); 2.58 (m, 1H, H_{14}); 2.23 (m, 1H, H_{9a}); 2.14 (m, 1H, $H_{5a\text{-pyranyl}}$); 2.07 (s, 3H, $COCH_3$), 2.03 (s, 3H, $COCH_3$); 2.02 (s, 3H, $COCH_3$); 1.93 (m,1H, $H_{5b\text{-pyranyl}}$); 1.89 (s, 3H, $COCH_3$); 1.87 (m, 1H, H_{9b}); 1.79 (m, 1H, H_8); 1.74 (2xs, 6H, $CH_{3\text{-}4,12}$); 1.22–1.32 (m, 3H, $H_{15a,\ 16,\ 17a}$); 1.23 (s, 3H, gem-CH_3); 1.19 (s, 3H, gem-CH_3); 1.13 (m, 1H, H_{17b}); 1.08 (m, 1H, H_{15b}); 0.96 (d, 3H, $CH_{3\text{-}6}$, J = 7 Hz); 0.93 (d, 3H, $CH_{3\text{-}15}$, J = 6.9 Hz); 0.82–0.87 (m, 9H, $CH_{3\text{-}8,16,18}$); MS-ESI *m*/*e* 908 (MH+, 50).

2.2. Recombinant Production of CXCL8 and Δ6 CXCL8 F17K F21K E70K N71K (dnCXCL8)

Construction of the expression plasmid, recombinant overexpression in *E. coli*, and the purification of these proteins have been described in detail elsewhere [37,38]. Proper protein folding was checked by the fluorescence emission maximum shift following chaotrope (6 M Gua.HCl) induced unfolding: a red shift of >5 nm was indicative for an intact overall fold of the CXCL8 proteins. In addition, far-UV CD spectra revealed the characteristic resonance bands of the CXCL8 proteins at 206 nm and 220 nm reflecting the existence of the α-helical and ß-sheet secondary structure elements.

2.3. Fluorescence Measurements and Data Analysis

As described before, isothermal fluorescence titration curves were recorded on a Perkin Elmer (Beaconsfield, UK) LS50B fluorometer [39]. In short, the emission of a 700 nM CXCL8 solution was recorded upon excitation at 280 nm over the range of 300–400 nm following the addition of an aliquot of the respective ligand and an equilibration period of 1 min. By this means, a concentration-dependent emission quenching and a red-shift in the fluorescence maximum were observed. The use of very concentrated ligand stock solutions ensured a dilution of the protein sample of less than 10%. The slit widths were set at 2 nm (700 nM CXCL8), and the spectra were recorded with 100 nm/min. A 290 nm cut-off filter was inserted into the emission path to avoid stray light. The samples were stirred during the measurements and the temperature was maintained at 22 °C by coupling to an external water bath. After background subtraction, the fluorescence intensity was integrated and the mean values resulting from three independent experiments were plotted against the volume-corrected concentration of the added ligand. The resulting isotherms were analyzed by non-linear regression using Origin 8.0 (Microcal Inc., Northampton, MA, USA) according to

$$F = \mathrm{Fi} + \mathrm{Fmax}\frac{\mathrm{Kd} + [\mathrm{protein}] + [\mathrm{ligand}] - \sqrt{\left(Kd + [protein] + [ligand]^2\right) - 4[protein][ligand]}}{2[protein]}$$

The quality of the fit was subsequently judged by the resulting R^2 value which was typically >95%.

2.4. Circular Dichroism Measurements and Analysis

The CD spectra of aqueous CXCL8 and CXCL8/ligand complex solutions were recorded in cuvettes with a path length of 0.1 cm on a Jasco J-710 spectropolarimeter (Japan Spectroscopic Co., Tokyo, Japan). Spectra were collected with a response time of 0.25 s and a data point resolution of 0.1 nm. Commonly, five scans were averaged to yield smooth spectra. The concentration of CXCL8 was held constant at 5 μM for all CD measurements. Mean residue ellipticities of the corrected spectra were calculated and plotted against the wavelength.

2.5. Heparan Sulfate Filter Binding Assays

An amount of 5 kcpm of tritium-labeled HS (Organon) was incubated in 10 mM phosphate buffer (pH 7.4) for one hour with 2 nmol CXCL8 and the competing ligand (heparin, PA501 or PA502) at the given concentrations. The protein/ligand complexes were trapped on a nitrocellulose filter (0.45 μm, Sartorius, Göttingen, Germany), and the filter was washed with 2 mL of incubation buffer. Protein-bound ligands were dissociated from the membrane by washing the filter with 2 mL of 2 M NaCl. The eluted radioactivity was determined and correlated with non-displaced ("bound") HS.

2.6. Preparation of Neutrophils

Neutrophils were isolated from whole blood collected from healthy Caucasian volunteers who had volunteered and provided informed consent. All blood donations were performed anonymously. Donors were screened according to internal criteria; however, no information regarding age, sex, or further demographics is available. Donor recruitment, informed consent, and ethical approval for the use of blood samples were managed in accordance with applicable regulatory standards ("No ethical approval is necessary as the study material is anonymous and voluntarily provided." according to the Declaration of Helsinki). Isolation was carried out using a Ficoll-Paque density gradient (Cytiva, Marlborough, MA, USA). Plasma and Ficoll fraction were aspirated down to the red blood cell pellet, and pellets were resuspended in up to twice of the original blood volume with HBSS −/− (Gibco). Red blood cells were mixed with a final concentration of 1% dextran solution. Cells settled for 1 h at RT without disturbing. The remaining red blood cells were lysed with ice-cold water, and neutrophils were washed several times with HBSS −/−.

2.7. Boyden Chamber Chemotaxis Assay

To investigate the chemotactic response of neutrophils to CXCL8, a 48-well Boyden chamber (Neuroprobe, Gaithersburg, MD, USA) and a polycarbonate membrane with a pore size of 5 μm (Neuroprobe) were used. The chemokine was placed in the lower compartment at a concentration of 0.15 μM) and isolated neutrophils were placed in the upper compartment to allow directed migration of immune cells through the porous membrane towards a chemokine gradient. The compounds PA501, PA502, and dnCXCL8 were added at the given concentrations to the lower chamber. Chambers were then incubated at 37 °C for 30 min in 5% CO_2. Subsequently, the membrane comprising the migrated cells was fixed with Hemocolor fixing solution (Merck) and stained with a Hemacolor staining kit (Merck). Migrated cells were counted under the microscope, and chemotactic indices were calculated, considering the background migration. All samples were measured in triplicates.

2.8. Transmigratory Assay

A Transwell assay was performed to test the modulatory effect of PA501 and PA502 on the transmigration of immune cells. A total of 35,000 EA.hy926 (ATCC® CRL-2922) cells per well were seeded on collagen-coated 96-well Transwell plates (96-well plate, polycarbonate

membrane with 5 µm pore size, Corning, New York, NY, USA) and grown for 48 h at 37 °C and 5% CO_2. Cells were stimulated for 4 h with 50 ng/mL TNFα. For the transmigration, 2×10^5 neutrophils were dispensed per well. Therefore 1×10^7 cells were isolated, diluted in 10 mL HBSS −/− each, and labeled with 10 µL of 2 mM Calcein AM (AM, Sigma) for 30 min at 37 °C and 5% CO_2. After labeling, cells were washed twice with HBSS −/−, and the pellet was resuspended in 4 mL 20 mM HEPES in HBSS +/+ (ThermoFisher, Waltham, MA, USA). Dilutions of 20 nM CXCL8 were pipetted into the lower wells. All samples were measured in triplicates. A total of 40 µL of cell suspension were mixed with 40 µL of the appropriate inhibitory agents at different concentrations and added to the upper wells, and the transmigration lasted for 2 h at 37 °C and 5% CO_2. Detection was performed by measuring the fluorescence intensity of migrated cells in the lower wells at 495 nm (excitation)/515 nm (emission) using the SpectraMax M3 Plate Reader (Molecular Devices, San Jose, CA, USA). Statistical analysis was performed with GraphPad v5.04 using Student's *t*-test. * $p < 0.05$, ** $p < 0.01$ and *** $p < 0.001$ were considered as statistically significant.

3. Results

We investigated in a prior study that the binding of the natural GAG ligands to wildtype CXCL8 depends upon the oligomerisation state of the chemokine as well as upon the GAG oligosaccharide chain length [38]. IFT can be used to explore biomolecular interactions by recording the change of the intrinsic chemokine fluorescence emission with respect to wavelength and intensity upon GAG binding and further calculating Kd values from the obtained binding isotherms. A concentration-dependent shift in the fluorescence emission characteristics—maximum wavelength shift and quenching—was detected following binding of GAGs due to the tryptophan chromophore positioned near the C-terminal α-helix, the suggested location of interaction with GAGs. Within the scope of this study, the binding of PA501 and PA502 to wildtype CXCL8 and its dominant-negative mutant (dnCXCL8) was investigated by isothermal fluorescence titrations giving Kd values of $4.6 \pm 0.8 \times 10^{-6}$ M and $4.2 \pm 0.6 \times 10^{-6}$ M, respectively for the wildtype chemokine (see Figure 2A,B). The obtained Kd values for the mutant chemokine were 2-fold (PA501) and 4-fold (PA502) higher, indicating a lower binding affinity of the compounds to the CXCL8 mutant compared to the wildtype (Figure 2). Considering that the binding affinity for the natural GAG ligands is increased following mutagenesis (see Figure 2C,D), the reverse behavior of PA501 and PA502 refers to a (partially) different chemokine binding site for these compounds compared to the natural HS ligand. Interestingly, the affinity of low-molecular-weight heparin (LMW heparin) to wildtype CXCL8 was found to be in a similar range as for the two polyketide-pyrone compounds (Figure 2).

Far-UV CD denotes the chiral molecules' varying absorption of the right- and left-handed components of circularly polarized light, resulting in elliptical polarization. This conformational effect was also reflected in the far-UV CD spectra of CXCL8 in complex with the two synthetic compounds (Figure 3). Compared to the unliganded chemokine, PA501 caused a more significant loss of the protein's secondary structure than PA502. This correlates well with the higher fractional saturation found for PA501 in the fluorescence isothermal titration experiments (see $-\Delta F/F_0$ values in Figure 2 referring to the fractional saturation of binding sites on the protein). It should, however, be noted that a fluorescence quenching and shift relates rather to changes in the tertiary structure of the protein, whereas differences in the far-UV spectra reflect changes in the secondary structure of the chemokine. In addition, it was found that the secondary structural change induced by PA502 closely resembled the conformational change induced by HS. The binding of both compounds did not lead to denaturation of the chemokine (like the addition of chaotrope, see insert in Figure 3).

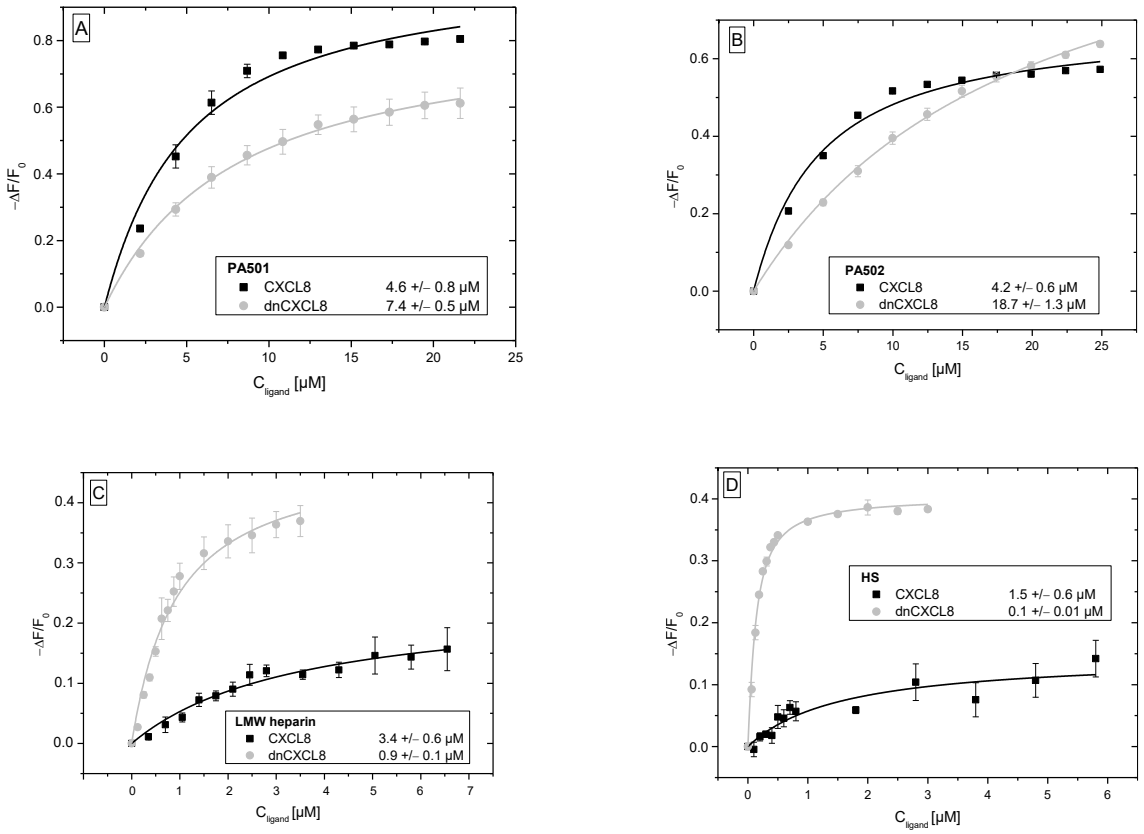

Figure 2. Fluorescence binding isotherms of (**A**) PA501, (**B**) and PA502, (**C**) LMW Heparin (low-molecular-weight heparin, average molecular weight of 8 kDa), and (**D**) Heparan sulphate (average molecular weight of 40 kDa) interacting with dimeric CXCL8 (700 nM) [40] and dnCXCL8 (700 nM). Inserts show the respective Kd values resulting for the non-linear fit (according equation in Section 2.3) of the bi-molecular interaction curve.

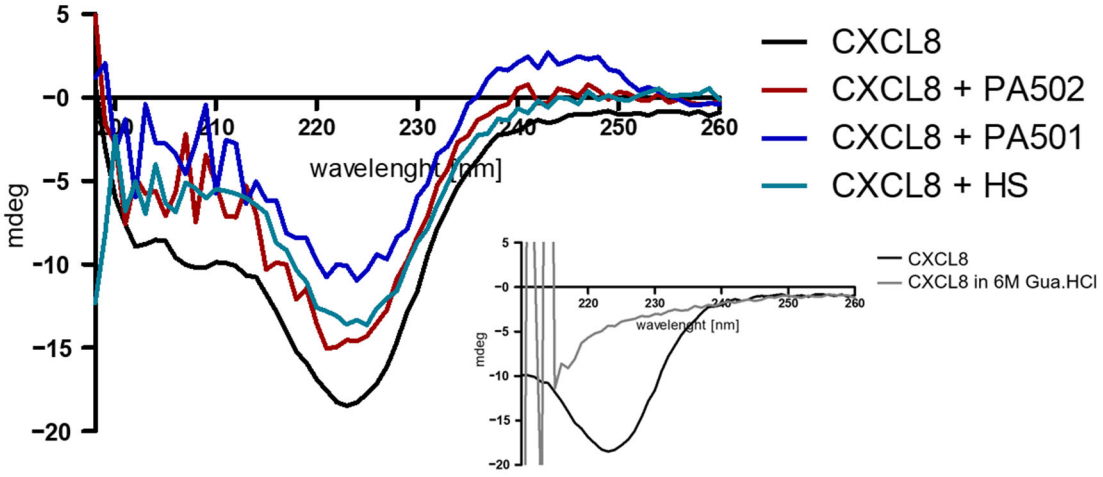

Figure 3. Far-UV CD spectra of CXCL8 compared with the molecular complexes of CXCL8/PA502, CXCL8/PA501, and CXCL8/HS. Insert: far-UV spectra of native CXCL8 compared with chaotrope (Gua.HCl)-unfolded CXCL8.

In order to investigate whether the two synthetic compounds can compete with the natural ligand, HS, for CXCL8 binding, filter binding assays were performed. In Figure 4, the displacement curves for radioactively labeled HS bound to CXCL8 are displayed. The two compounds were found to differ significantly in their ability to compete with HS for CXCL8 binding. PA501 gave an IC_{50} value of $<1 \times 10^{-4}$ M, whereas PA502 yielded IC_{50}

values of 5.4×10^{-4} M. Heparin, despite being a direct structural relative of HS and its higher sulfation content, depicts an IC_{50} value around 900 µM and is thus an unexpectedly less efficient competitor for HS bound to CXCL8 than these two compounds.

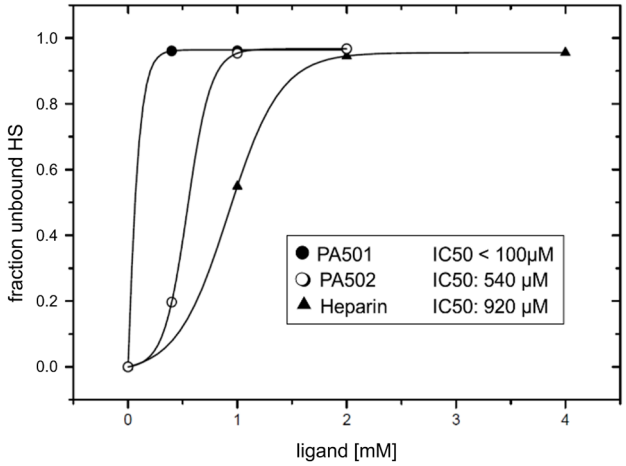

Figure 4. Filter binding assays of heparin (▲), PA502 (○), and PA501 (●) displacing radio-actively labeled HS from CXCL8.

To investigate if the two synthetic compounds displaced HS from CXCL8 by competing for the same or similar or partly overlapping binding site(s), or if an allosteric effect was responsible for HS displacement, the truncation mutant chemokine $CXCL8_{1-58}$ was considered. This mutant was previously shown to be monomeric, chemotactically fully active [41], and to adopt a similar structure as wildtype CXCL8 [42]. In addition, the C-terminal helix of CXCL8 was found to be responsible for GAG binding [29]. Therefore, a truncation mutant lacking this part of the molecule was expected to shed some light on the binding sites of the natural HS ligand and the synthetic compounds. Since the intrinsic tryptophan fluorophore at position 57 was contained in $CXCL8_{1-58}$, fluorescence isothermal titration experiments using intrinsic emission changes could be performed (Figure 5).

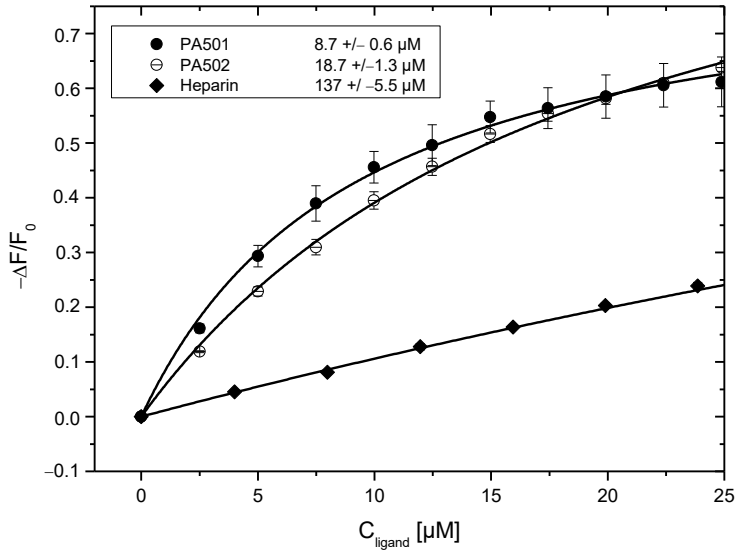

Figure 5. Fluorescence binding isotherms of heparin (◆), PA502 (○) and PA501 (●) interacting with $CXCL8_{1-58}$ (700 nM). The insert shows the respective Kd values resulting for the non-linear fit (according equation in Section 2.3) of the bi-molecular interaction curve.

Heparin, which bound to full-length CXCL8 with similar affinity as PA501 and PA502, interacted with the N-terminally truncated mutant $CXCL8_{1-58}$ only in a very low-affinity and non-specific way (hence the flat bi-molecular interaction curve shown in Figure 5). The affinities found for the two synthetic compounds, on the other hand, were significantly higher, giving Kd values of 8.7×10^{-6} M (PA501) and 18.7×10^{-6} M (PA502) for $CXCL8_{1-58}$. Based on these data we derive that the synthetic compounds potentially use the second binding site on CXCL8 and that PA501 is using this site more efficiently than PA502, which is also reflected in the IC_{50} values from the HS displacement experiments (Figure 4). Thus, the C-terminal α-helix of CXCL8, which is mainly responsible for GAG binding, is used only partly for the interaction with the two synthetic compounds PA501 and PA502.

Next, we were interested in a potential inhibitory effect of PA501 and PA502 on CXCL8-induced neutrophil mobilization. For this purpose, the impact of the two compounds on CXCL8-induced neutrophil chemotaxis was investigated in a Boyden chamber set-up (in comparison to dnCXCL8 which was shown to be active in several mouse models for the treatment of neutrophilic inflammation [33,34,36,43]). As is shown in Figure 6. The two compounds PA501 and PA502 were found to promote chemotaxis, as has been similarly published for HS by Webb et al. [44].

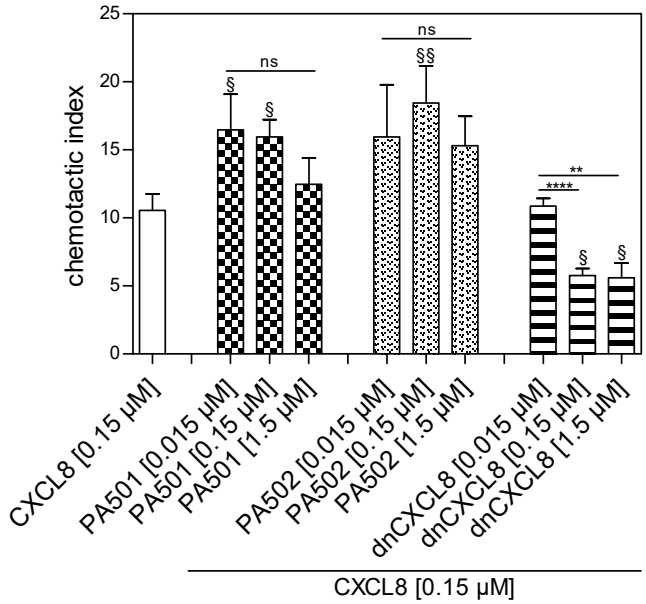

Figure 6. CXCL8-induced chemotaxis of human neutrophils. * indicates significant differences within the groups, ns indicates non-significant, § and §§ indicate significance with respect to the CXCL8 control (unpaired *t*-test, two-tailed confidence interval 95%,* $p < 0.05$, ** $p < 0.01$, *** $p < 0.001$, **** $p < 0.0001$).

In order to expand into a two cellular system, i.e., considering neutrophils and endothelial cells, we moved to a transmigratory assay to characterize the two compounds PA501 and PA502 further with respect to their impact on CXCL8-induced neutrophil chemotaxis. Both synthetic compounds significantly inhibited the mobilization and transmigration of neutrophils in response to CXCL8. PA501 was found to be more effective, yielding decreased transmigration at all tested concentrations (see Figure 7D).

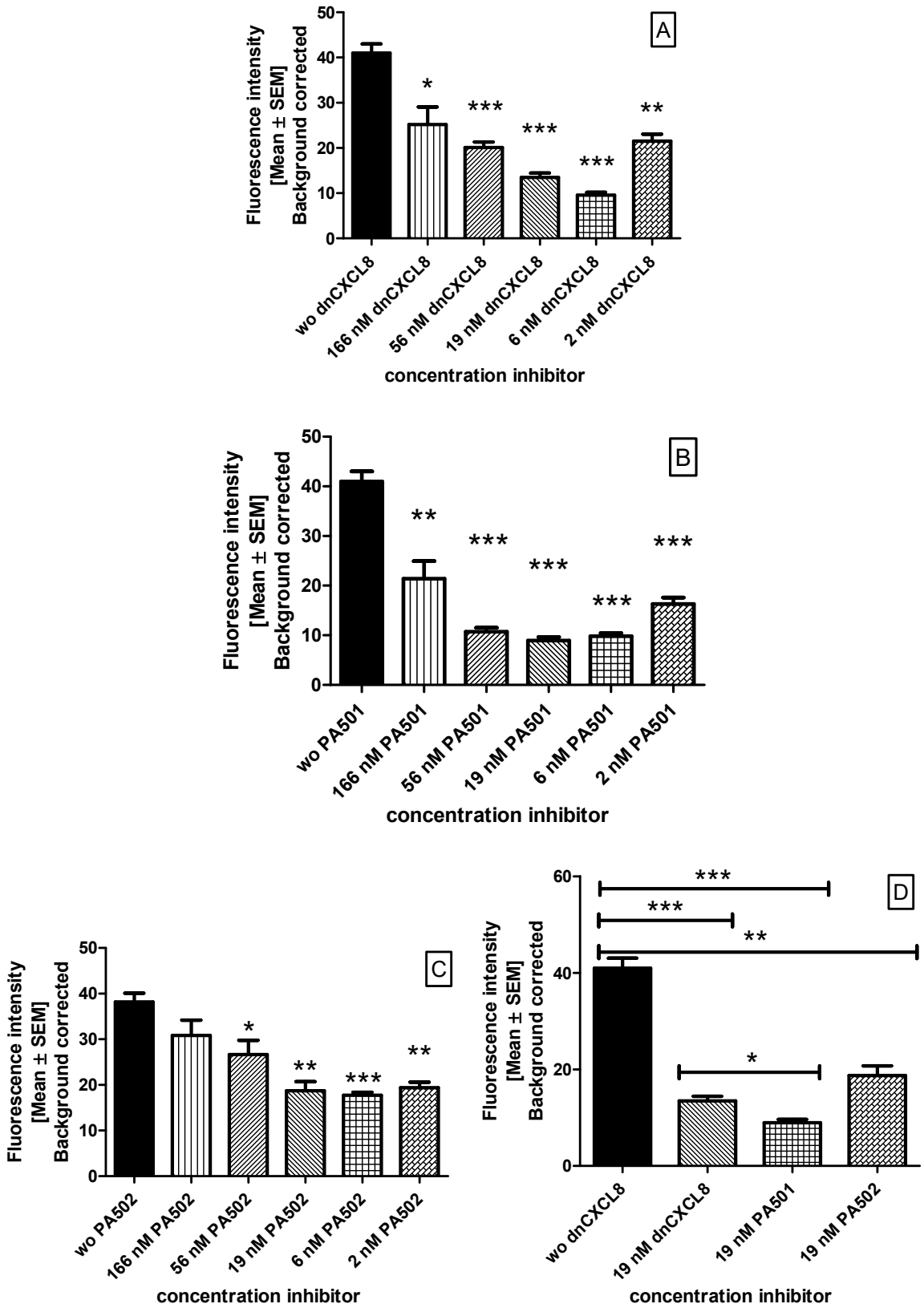

Figure 7. Transmigration of neutrophils towards CXCL8, inhibited with (**A**) dnCXCL8, (**B**) PA501, (**C**) PA502, and (**D**) compared inhibitory effect of these 3 substances at 19 nM concentration. (**A**–**C**) Transmigration was compared to migration without inhibitor using Student's *t*-test. * $p < 0.05$, ** $p < 0.01$ *** $p < 0.001$ was considered as statistically significant. (**D**) compares 19 nM dnCXCL8 migration to PA compounds using Student's *t*-test. * $p < 0.05$, ** $p < 0.01$ *** $p < 0.001$

dnCXCL8 and the compounds PA501 and PA502 interfere at the same pathological axis, i.e., the chemokine-GAG binding interface. dnCXCL8 competes with CXCL8 for its cognate GAG binding site and can thus be viewed as a protein-based GAG antagonist. On the other hand, the two synthetic compounds bind to the GAG binding site (and potentially additional sites) of the chemokine thereby interfering with natural GAG interactions. Interestingly, the three molecules were found to exhibit different dose–response profiles (Figure 7) with the lowest efficiacy found for PA502. Common to the cell-based activities is the inverse bell-shape dose–response for which the two binding sites serve as an explanatory model (see Discussion below).

4. Discussion

The interaction of chemokines and their G-protein-coupled receptors on the surface of immune cells has been extensively investigated. It certainly plays an essential role in immune cell mobilization and migration during acute and chronic inflammatory processes. Glycosaminoglycans like heparan sulfate (HS) exhibit specific sulfation patterns, depending upon the site of their expression, with which certain basic amino acid patterns on chemokines interact to be attracted to the site of inflammation. In addition, the interaction with GAGs protects chemokines from degradation and induces protein oligomerization thereby amplifying the chemokine's activity. Targeting the chemokine–GAG interaction is therefore seen as a powerful strategy for treating chemokine-related diseases. Only a few approaches to therapeutically target chemokine–GAG interactions have been pursued so far. We have developed a dominant-negative mutant of CXCL8 that has increased GAG binding affinity and, in addition, an inactivated GPC-receptor function which was shown to displace the wildtype chemokine from cell-surface GAGs and to reduce immune cells in the chronically inflamed tissue [33,34,36,40]. Here we have investigated a novel therapeutical route targeting the same CXCL8-GAG interaction interface.

Two polyketide-pyrone compounds, PA501 and PA502, were synthesized and Kd values were determined using isothermal fluorescence titration. Both compounds bound to CXCL8 with 2.5 times lower affinity compared to the natural ligand HS, but they interestingly exhibited a similar affinity as low-molecular-weight (LMW) heparin. Although the Kd values for both substances were almost identical, the fractional saturation, as expressed in the limiting values of $-\Delta F/F0$ upon saturation (see Figure 2), differed significantly among the two compounds. This means that the intrinsic fluorescence of CXCL8 becomes less, though still in a concentration-dependent manner, quenched upon binding of PA502 compared to PA501. PA501 and PA502 can thus be assumed to exert a different structural change of the chemokine, giving a different microenvironment for the intrinsic tryptophan fluorophore resulting in different fluorescence quenching.

Far-UV circular dichroism experiments were performed to further analyze the difference in conformational rearrangements following the binding of the synthetic compounds to CXCL8 compared to unliganded CXCL8. Changes of the chemokine's secondary structure were more pronounced with PA501 than with PA502 (see Figure 3), contrasting their similar binding affinities (see Figure 2). We therefore assume that PA501 has a greater structural impact on CXCL8 than PA502, independently of the interaction strength. In filter binding assays, the potency of the two PA compounds to displace the natural ligand HS from CXCL8 was investigated (see Figure 4). The IC_{50} values of PA501 and PA502 were found to be significantly different, with PA501 being the better competitor, which is in contrast to the similar dissociation constants of the two compounds. The broader structural effect of PA501 induced by binding to CXCL8 compared to PA502 (see Figure 3) is apparently responsible for the more efficient displacement potency of PA501. This broad conformational impact of the binding of the two PA compounds also became apparent from

the binding domain occupied by the two synthetic compounds compared to the natural HS ligand: binding of the GAG lingand is dependent upon the presence of the C-terminal α-helix of the chemokine, whereas PA501 and PA502 were still able to bind to the truncation mutant $CXCL8_{1\text{-}58}$ which lacks the C-terminus. PA501 was found to be the ligand with an approximately two-times-higher affinity for the truncation mutant than PA502, which can be attributed to the larger structural induced fit of CXCL8 following PA501 binding. Two binding sites on CXCL8 for GAGs were already identified in 1998 by Kuschert et al. [32] using a combination of site-directed mutagenesis and NMR spectroscopy. These authors identified a heparin-binding surface on CXCL8 that includes the C-terminal α-helix and the proximal loop around residues 18–23. The heparin-binding site is spatially partially overlapping with residues involved in GPC receptor binding.

Finally, the synthetic compounds have been investigated for their inhibitory potency on CXCL8-induced neutrophil activation/mobilization as well as on transendothelial neutrophil migration. In the Boyden chamber experiments we discovered that the two compounds PA501 and PA502 promote chemotaxis independently upon compound concentration (see Figure 6), as has similarly been published by Webb et al. [44] for HS. This was interpreted as allosteric induction of the GPC receptor (CXCR1/2) binding domain of the chemokine. In a transwell set-up, on the other hand, in which endothelial cells—mimicking the vessel wall—are present in addition to the neutrophils, an inverse bell-shaped inhibitory dose response was found (see Figure 7). Here it must be noted that neutrophil cell activation/migration was inhibited to a certain degree by PA501, and by PA502 at most concentrations regarded in this study (see Figure 7B,C). The inverse-shaped dose response can be explained by the different occupation of the two different binding sites on CXCL8 for PA501 and PA502—the two different binding sites exhibiting different affinities (see Figure 5). At high compound concentrations, both binding sites are occupied but the chemotactic-activating site dominates, i.e., an active conformation of the chemokine is induced which promotes GPC receptor binding and activation. At lower compound concentrations, the second binding site, which is the actual GAG binding site with higher affinity for the compounds (and GAGs), can become populated leading to GAG competition and thus to inhibition of neutrophil chemotaxis. Differences found for the two synthetic compounds are preliminarily pointing in different recognition/binding specificities, which will be explored further in the future. Moreover, before fueling the two compounds into a regular drug development strategy, further pharmacological data must be generated. Particularly since the two compound classes, PA501 and PA502 and dnCXCL8, represent two entirely different potential pro-drugs: low-molecular-weight synthetic compounds on the one hand, and a biotechnologically derived biologic on the other. The application route and in vivo pharmacology of dnCXCL8 have been studied intensively in the past and have already been published [34,35] in our manuscript. For PA501 and PA502, corresponding in vivo pharmacological data will be collected in the future and will be prepared for publication in a follow-up manuscript. A potential advantage of PA501 and PA502, however, could be their oral bioavailability.

Author Contributions: Conceptualization, A.J.K.; methodology, T.G. and P.P.; validation, T.G.; formal analysis, P.P.; investigation, T.G., P.P., B.M. and K.T.; writing—original draft preparation, T.G. and B.M.; writing—review and editing, P.P. and A.J.K.; visualization, T.G., supervision, A.J.K.; project administration, A.J.K. All authors have read and agreed to the published version of the manuscript.

Funding: The authors acknowledge the financial support by the University of Graz.

Data Availability Statement: Upon request, data are available from the corresponding author.

Acknowledgments: The authors acknowledge the technical support by members of the University of Manchester. Open Access Funding by the University of Graz.

Conflicts of Interest: The authors declare no conflicts of interest. A.J.K. is co-founder and CEO of Antagonis Biotherapeutics GmbH.

References

1. Mukaida, N.; Harada, A.; Matsushima, K. A novel leukocyte chemotactic and activating cytokine, interleukin-8 (IL-8). In *Cytokines: Interleukins and Their Receptors*; Springer: Berlin/Heidelberg, Germany, 1995; pp. 261–287.
2. Baggiolini, M.; Loetscher, P. Chemokines in inflammation and immunity. *Immunol. Today* **2000**, *21*, 418–420. [CrossRef]
3. Matsushima, K.; Morishita, K.; Yoshimura, T.; Lavu, S.; Kobayashi, Y.; Lew, W.; Appella, E.; Kung, H.F.; Leonard, E.J.; Oppenheim, J.J. Molecular cloning of a human monocyte-derived neutrophil chemotactic factor (MDNCF) and the induction of MDNCF mRNA by interleukin 1 and tumor necrosis factor. *J. Exp. Med.* **1988**, *167*, 1883–1893. [CrossRef]
4. Baggiolini, M.; Dewald, B.; Moser, B. Human chemokines: An update. *Annu. Rev. Immunol.* **1997**, *15*, 675–705. [CrossRef]
5. Mukaida, N.; Harada, A.; Matsushima, K. Interleukin-8 (IL-8) and monocyte chemotactic and activating factor (MCAF/MCP-1), chemokines essentially involved in inflammatory and immune reactions. *Cytokine Growth Factor Rev.* **1998**, *9*, 9–23. [CrossRef]
6. Luster, A.D. Chemokines—Chemotactic Cytokines That Mediate Inflammation. *N. Engl. J. Med.* **1998**, *338*, 436–445. [CrossRef] [PubMed]
7. Mishra, A.; Suman, K.H.; Nair, N.; Majeed, J.; Tripathi, V. An updated review on the role of the CXCL8-CXCR1/2 axis in the progression and metastasis of breast cancer. *Mol. Biol. Rep.* **2021**, *48*, 6551–6561. [CrossRef]
8. Richardson, R.M.; Marjoram, R.J.; Barak, L.S.; Snyderman, R. Role of the cytoplasmic tails of CXCR1 and CXCR2 in mediating leukocyte migration, activation, and regulation. *J. Immunol.* **2003**, *170*, 2904–2911. [CrossRef] [PubMed]
9. Bizzarri, C.; Beccari, A.R.; Bertini, R.; Cavicchia, M.R.; Giorgini, S.; Allegretti, M. ELR+ CXC chemokines and their receptors (CXC chemokine receptor 1 and CXC chemokine receptor 2) as new therapeutic targets. *Pharmacol. Ther.* **2006**, *112*, 139–149. [CrossRef]
10. Brat, D.J.; Bellail, A.C.; Van Meir, E.G. The role of interleukin-8 and its receptors in gliomagenesis and tumoral angiogenesis. *Neuro. Oncol.* **2005**, *7*, 122–133. [CrossRef] [PubMed]
11. Frevert, C.W.; Kinsella, M.G.; Vathanaprida, C.; Goodman, R.B.; Baskin, D.G.; Proudfoot, A.; Wells, T.N.; Wight, T.N.; Martin, T.R. Binding of interleukin-8 to heparan sulfate and chondroitin sulfate in lung tissue. *Am. J. Respir. Cell Mol. Biol.* **2003**, *28*, 464–472. [CrossRef]
12. Proudfoot, A.E. The biological relevance of chemokine-proteoglycan interactions. *Biochem. Soc. Trans.* **2006**, *34*, 422. [CrossRef]
13. Rudd, T.; Skidmore, M.; Guerrini, M.; Hricovini, M.; Powell, A.; Siligardi, G.; Yates, E. The conformation and structure of GAGs: Recent progress and perspectives. *Curr. Opin. Struct. Biol.* **2010**, *20*, 567–574. [CrossRef] [PubMed]
14. Yates, E.A.; Rudd, T.R. Recent innovations in the structural analysis of heparin. *Int. J. Cardiol.* **2016**, *212*, S5–S9. [CrossRef] [PubMed]
15. Gandhi, N.S.; Mancera, R.L. The structure of glycosaminoglycans and their interactions with proteins. *Chem. Biol. Drug Des.* **2008**, *72*, 455–482. [CrossRef]
16. Sodhi, H.; Panitch, A. Glycosaminoglycans in tissue engineering: A review. *Biomolecules* **2021**, *11*, 29. [CrossRef]
17. Vallet, S.D.; Clerc, O.; Ricard-Blum, S. Glycosaminoglycan–Protein Interactions: The First Draft of the Glycosaminoglycan Interactome. *J. Histochem. Cytochem.* **2021**, *69*, 93–104. [CrossRef]
18. Lindahl, U.; Couchman, J.; Kimata, K.; Esko, J.D. Proteoglycans and sulfated glycosaminoglycans. In *Essentials of Glycobiology*; Cold Spring Harbor Laboratory Press: Cold Spring Harbor, NY, USA, 2017.
19. Reitsma, S.; Slaaf, D.W.; Vink, H.; van Zandvoort, M.A.; Oude Egbrink, M.G. The endothelial glycocalyx: Composition, functions, and visualization. *Pflügers Arch.-Eur. J. Physiol.* **2007**, *454*, 345–359. [CrossRef] [PubMed]
20. Pries, A.R.; Secomb, T.W.; Gaehtgens, P. The endothelial surface layer. *Pflügers Arch.* **2000**, *440*, 653–666. [CrossRef]
21. Kolset, S.O.; Prydz, K.; Pejler, G. Intracellular proteoglycans. *Biochem. J.* **2004**, *379*, 217–227. [CrossRef]
22. Handel, T.M.; Johnson, Z.; Crown, S.E.; Lau, E.K.; Sweeney, M.; Proudfoot, A.E. Regulation of Protein Function by Glycosaminoglycans—As exemplified by Chemokines. *Annu. Rev. Biochem.* **2005**, *74*, 385–410. [CrossRef]
23. Mulloy, B.; Forster, M.J. Conformation and dynamics of heparin and heparan sulfate. *Glycobiology* **2000**, *10*, 1147–1156. [CrossRef]
24. Mulloy, B.; Rider, C. Cytokines and proteoglycans: An introductory overview. *Biochem. Soc. Trans.* **2006**, *34*, 409–413. [CrossRef]
25. Laremore, T.N.; Zhang, F.; Dordick, J.S.; Liu, J.; Linhardt, R.J. Recent progress and applications in glycosaminoglycan and heparin research. *Curr. Opin. Chem. Biol.* **2009**, *13*, 633–640. [CrossRef]
26. Lindahl, U.; Kusche-Gullberg, M.; Kjellén, L. Regulated diversity of heparan sulfate. *J. Biol. Chem.* **1998**, *273*, 24979–24982. [CrossRef] [PubMed]
27. Stringer, S.E.; Kandola, B.S.; Pye, D.A.; Gallagher, J.T. Heparin sequencing. *Glycobiology* **2003**, *13*, 97–107. [CrossRef] [PubMed]
28. Gallagher, J. Fell-Muir Lecture: Heparan sulphate and the art of cell regulation: A polymer chain conducts the protein orchestra. *Int. J. Exp. Pathol.* **2015**, *96*, 203–231. [CrossRef]
29. Spillmann, D.; Witt, D.; Lindahl, U. Defining the interleukin-8-binding domain of heparan sulfate. *J. Biol. Chem.* **1998**, *273*, 15487–15493. [CrossRef]

30. Rek, A.; Krenn, E.; Kungl, A. Therapeutically targeting protein–glycan interactions. *Br. J. Pharmacol.* **2009**, *157*, 686–694. [CrossRef]
31. Rek, A.; Geretti, E.; Goger, B.; Kungl, A.J. The biophysics of chemokine/glycosaminoglycan interactions. In *Recent Research Developments in Biophysics and Biochemistry*; Research Signpost: Kerala, India, 2002; pp. 319–340.
32. Kuschert, G.S.; Hoogewerf, A.J.; Proudfoot, A.E.; Chung, C.W.; Cooke, R.M.; Hubbard, R.E.; Wells, T.N.; Sanderson, P.N. Identification of a glycosaminoglycan binding surface on human interleukin-8. *Biochemistry* **1998**, *37*, 11193–11201. [CrossRef]
33. Gschwandtner, M.; Strutzmann, E.; Teixeira, M.M.; Anders, H.J.; Diedrichs-Mohring, M.; Gerlza, T.; Wildner, G.; Russo, R.C.; Adage, T.; Kungl, A.J. Glycosaminoglycans are important mediators of neutrophilic inflammation in vivo. *Cytokine* **2017**, *91*, 65–73. [CrossRef] [PubMed]
34. Adage, T.; del Bene, F.; Fiorentini, F.; Doornbos, R.P.; Zankl, C.; Bartley, M.R.; Kungl, A.J. PA401, a novel CXCL8-based biologic therapeutic with increased glycosaminoglycan binding, reduces bronchoalveolar lavage neutrophils and systemic inflammatory markers in a murine model of LPS-induced lung inflammation. *Cytokine* **2015**, *76*, 433–441. [CrossRef]
35. Adage, T.; Konya, V.; Weber, C.; Strutzmann, E.; Fuchs, T.; Zankl, C.; Gerlza, T.; Jeremic, D.; Heinemann, A.; Kungl, A.J. Targeting glycosaminoglycans in the lung by an engineered CXCL8 as a novel therapeutic approach to lung inflammation. *Eur. J. Pharmacol.* **2015**, *748*, 83–92. [CrossRef]
36. McElvaney, O.J.; O'Reilly, N.; White, M.; Lacey, N.; Pohl, K.; Gerlza, T.; Bergin, D.A.; Kerr, H.; McCarthy, C.; O'Brien, M.E. The effect of the decoy molecule PA401 on CXCL8 levels in bronchoalveolar lavage fluid of patients with cystic fibrosis. *Mol. Immunol.* **2015**, *63*, 550–558. [CrossRef]
37. Falsone, A.; Wabitsch, V.; Geretti, E.; Potzinger, H.; Gerlza, T.; Robinson, J.; Adage, T.; Teixeira, M.M.; Kungl, A.J. Designing CXCL8-based decoy proteins with strong anti-inflammatory activity in vivo. *Biosci. Rep.* **2013**, *33*, 743–754. [CrossRef] [PubMed]
38. Goger, B.; Halden, Y.; Rek, A.; Mosl, R.; Pye, D.; Gallagher, J.; Kungl, A.J. Different affinities of glycosaminoglycan oligosaccharides for monomeric and dimeric interleukin-8: A model for chemokine regulation at inflammatory sites. *Biochemistry* **2002**, *41*, 1640–1646. [CrossRef] [PubMed]
39. Gerlza, T.; Hecher, B.; Jeremic, D.; Fuchs, T.; Gschwandtner, M.; Falsone, A.; Gesslbauer, B.; Kungl, A.J. A Combinatorial Approach to Biophysically Characterise Chemokine-Glycan Binding Affinities for Drug Development. *Molecules* **2014**, *19*, 10618–10634. [CrossRef]
40. Horcher, M.; Rot, A.; Aschauer, H.; Besemer, J. IL-8 derivatives with a reduced potential to form homodimers are fully active in vitro and in vivo. *Cytokine* **1998**, *10*, 1–12. [CrossRef] [PubMed]
41. Clark-Lewis, I.; Schumacher, C.; Baggiolini, M.; Moser, B. Structure-activity relationships of interleukin-8 determined using chemically synthesized analogs. Critical role of NH2-terminal residues and evidence for uncoupling of neutrophil chemotaxis, exocytosis, and receptor binding activities. *J. Biol. Chem.* **1991**, *266*, 23128–23134. [CrossRef] [PubMed]
42. Sticht, H.; Auer, M.; Schmitt, B.; Besemer, J.; Horcher, M.; Kirsch, T.; Lindley, I.J.; Rösch, P. Structure and activity of a chimeric interleukin-8-melanoma-growth-stimulatory-activity protein. *Eur. J. Biochem.* **1996**, *235*, 26–35. [CrossRef] [PubMed]
43. Bedke, J.; Nelson, P.J.; Kiss, E.; Muenchmeier, N.; Rek, A.; Behnes, C.L.; Gretz, N.; Kungl, A.J.; Grone, H.J. A novel CXCL8 protein-based antagonist in acute experimental renal allograft damage. *Mol. Immunol.* **2010**, *47*, 1047–1057. [CrossRef] [PubMed]
44. Webb, L.M.; Ehrengruber, M.U.; Clark-Lewis, I.; Baggiolini, M.; Rot, A. Binding to heparan sulfate or heparin enhances neutrophil responses to interleukin 8. *Proc. Natl. Acad. Sci. USA* **1993**, *90*, 7158–7162. [CrossRef] [PubMed] [PubMed Central]

Disclaimer/Publisher's Note: The statements, opinions and data contained in all publications are solely those of the individual author(s) and contributor(s) and not of MDPI and/or the editor(s). MDPI and/or the editor(s) disclaim responsibility for any injury to people or property resulting from any ideas, methods, instructions or products referred to in the content.